



HAL
open science

Oxide-Supported Titanium Catalysts: Structure–Activity Relationship in Heterogeneous Catalysis, with the Choice of Support as a Key Step

Cherif Larabi, Sébastien Norsic, Lhoussain Khrouz, Olivier Boyron, Kai
Chung Szeto, Christine Lucas, Mostafa Taoufik, Aimery De mallmann

► **To cite this version:**

Cherif Larabi, Sébastien Norsic, Lhoussain Khrouz, Olivier Boyron, Kai Chung Szeto, et al..
Oxide-Supported Titanium Catalysts: Structure–Activity Relationship in Heterogeneous Cataly-
sis, with the Choice of Support as a Key Step. *Organometallics*, 2020, 39 (24), pp.4608-4617.
10.1021/acs.organomet.0c00650 . hal-03375404

HAL Id: hal-03375404

<https://hal.science/hal-03375404>

Submitted on 12 Oct 2021

HAL is a multi-disciplinary open access archive for the deposit and dissemination of scientific research documents, whether they are published or not. The documents may come from teaching and research institutions in France or abroad, or from public or private research centers.

L'archive ouverte pluridisciplinaire **HAL**, est destinée au dépôt et à la diffusion de documents scientifiques de niveau recherche, publiés ou non, émanant des établissements d'enseignement et de recherche français ou étrangers, des laboratoires publics ou privés.

Oxide Supported Titanium Catalysts: Structure Activity Relationship in Heterogeneous Catalysis, with the Choice of the Support as a Key Step.

Cherif Larabi,* Sébastien Norsic, Lhoussain Khrouz,# Olivier Boyron, Kai Chung Szeto, Christine Lucas, Mostafa Taoufik* and Aimery De Mallmann*

Université de Lyon, ESCPE Lyon, UMR 5265 CNRS, Université Claude Bernard Lyon 1, Laboratoire C2P2, 43 bd du 11 Novembre 1918, F-69626 Villeurbanne Cedex, France.

Université de Lyon, ENS de Lyon, CNRS UMR 5182, Université Claude Bernard Lyon 1, Laboratoire de Chimie, 46 Allée d'Italie, 69342, Lyon, France

RECEIVED DATE (to be automatically inserted after your manuscript is accepted if required according to the journal that you are submitting your paper to)

Abstract:

The reactions of tetrakis-neopentyl titanium, TiNp_4 (1), with the surface of three solid oxides, silica, silica-alumina, and alumina, all partially dehydroxylated at 500 °C under vacuum were achieved. The resulting supported organometallic species react with dihydrogen to form the corresponding supported hydrides. The preparation of supported titanium hydrides on alumina is described here in detail, and the species obtained were extensively characterized by FTIR, solid state NMR and EPR spectroscopy and mass-balance analysis. The supported titanium hydride species were tested in three important reactions for petrochemistry: epoxidation of 1-octene, depolymerization of Fischer-Tropsch waxes and polymerization of ethylene. The activities of titanium hydrides supported on alumina were compared to their silica and silica-alumina supported analogues.

Introduction.

Typical heterogeneous catalysts are solid phases or consist of active species (inorganic clusters or metal-organic complexes) immobilized on solid supports such as silica,¹ alumina,² clay,³ zeolite,⁴ etc. Commercial heterogeneous catalysts suffer from the presence of different and ill-defined active sites, due to the heterogeneity of the surface and lack of controlled preparation procedure at the molecular level. Fundamental understandings of the active sites and their coordination spheres are essential in order to develop next generation catalysts with enhanced activities and selectivities. An alternative approach to prepare molecularly well-defined species on a support has been proposed: Surface Organometallic Chemistry.⁵ Generally, this methodology offers access to well-defined active sites on a solid surface. Moreover, the interactions between the support and the active center, as well as the mechanism of the catalytic reaction, can be elucidated by standard spectroscopic methods very similarly to the case of homogeneous catalysis.⁶ As a consequence, an opportunity to tune the catalytic site reactivity (coordination sphere: supports, ligands) toward a given reaction arises. Several essential catalytic systems for processes such as alkene metathesis,⁷⁻⁹ imine metathesis,¹⁰ controlled depolymerization of waxes,^{11,12} methane coupling,^{13,14} alkane dehydrogenation,^{15,16} alkane aromatization,^{17,18} 2-butene dimerization,¹⁹ alkene epoxidation²⁰ have been demonstrated using this strategy. Importantly, catalysts prepared by this approach have also led to the discovery of new reactions, unknown in homogeneous catalysis, such as alkane metathesis,²¹ direct conversion of ethylene to propylene,²² and metathetic oxidation.²³ The work of Basset, a pioneer of surface organometallic chemistry, has exhaustively reviewed the preparation and characterization of the highly reactive early -transition -metal hydride species, supported on various oxides.^{5,24}

Among all investigated transition -metal systems, supported Ti species with adequately tuned coordination spheres were shown to play an important role in epoxidation,^{25,26} hydroamination,²⁷ catalytic imido transfer,²⁸ polymerization,²⁹ and depolymerization processes.^{11,12} Nevertheless, a detailed description of the surface Ti species remains still difficult to access. Previously, it has been suggested that a proper choice of the dehydroxylation temperature of the support allows control of the distribution of surface hydroxyl groups and tuning their chemical reactivity.⁵ As a result, when they react with organometallic compounds, such as tetrakis-neopentyl titanium, mono or bis coordinated Ti alkyl species can be selectively obtained, as a function of the surface silanol density.³⁰⁻³² A supported Ti hydride is a very important intermediate among the reactions mentioned. Precisely, in alkene epoxidation, it can

undergo protonolysis of the alkyl hydroperoxide, in polymerization, it could readily insert olefins, and in depolymerization, it can readily activate the long-chain hydrocarbon by σ -bond metathesis and cut C-C bonds by β -alkyl transfer.^{11,12} Hence, this work comprises an extensive study of Ti hydrides prepared on conventional supports. Previously, Ti hydrides supported on silica and silica-alumina have been reported.^{5,12} The major Ti hydride species is tris-coordinated to the surface, as revealed by IR, solid state NMR, mass balance analysis, EPR, stoichiometric reactivity analysis and XAS. The synthesis of the titanium hydride supported on alumina is presented here for the first time. These supported Ti hydride materials have been investigated for 1-octene epoxidation, ethylene polymerization and depolymerization of a Fischer-Tropsch wax (FT-wax).

Experimental section.

General Procedures. For the organometallic synthesis, experiments were carried out using standard Schlenk and glovebox techniques. Solvents were purified and dried according to standard procedures and stored over 3 Å molecular sieves. Ti(OEt)₄ (99%, Aldrich), ¹³CO₂ (99% ¹³C, Cambridge Isotopes), *t*BuMgCl (1.7 M in diethyl ether, Aldrich), LiAlH₄ (95%, Aldrich), MgSO₄ (Laurylab), NaHCO₃ (Prolabo), and Vilsmeier reagent (95%, Aldrich, stored under argon) were used as received. *t*BuCH₂Li was prepared from *t*BuCH₂Cl (98%, Lancaster) and Li wires (Aldrich). [Ti(CH₂*t*Bu)₄] was prepared according to the literature procedure.³³ ¹³C labeled [Ti(^{*}CH₂*t*Bu)₄] was prepared as already reported elsewhere.^{12,32}

A TBHP (*t*BuOOH) anhydrous solution in pentane was prepared according to the procedures reported by Sharpless *et al.*³⁴ from a commercial solution of 70% TBHP in water and stored under argon over 3 Å molecular sieves prior to use. 1-Octene and dodecane were provided from Aldrich and stored over molecular sieves (3 Å) under argon after purification on a neutral alumina and elimination of solved gases by the freeze-pump-thaw technique. *t*BuOH, 1,2-epoxyoctane, and 1,2-octanediol were used as received for the gas chromatographic peak identification and calibration. Isopropanol, acetic acid, sodium iodide, and sodium thiosulfate were used as is for the iodometric titration of the anhydrous solution of TBHP in pentane.³⁴

Analyses of organics (*t*BuOH, pentane, *t*BuOOH, 1-octene, 1,2-epoxyoctane and dodecane) were performed on a HP 6890 gas chromatograph, equipped with a flame ionization detector (FID) and a HP-1 column (30 m × 0.32 mm) with the following temperature program: 3 min at 70 °C, 20 °C min⁻¹ up to 200 °C and 5 min at 200 °C.

Gas-phase quantitative analyses of light alkanes (grafting, hydrogenolysis) were performed on a Hewlett-Packard 5890 Series II gas chromatograph equipped with a flame ionization detector and an Al₂O₃/KCl on fused silica column (50 m × 0.32 mm). The amount of dihydrogen evolved (protonolysis with *t*BuOH) was determined with a Hewlett-Packard 6890 gas chromatograph equipped with a TCD detector and a molecular sieve column (15 m × 0.32 mm).

Infrared spectra were recorded on a Nicolet FT-IR Magna 550 spectrometer equipped with a cell designed for in situ preparations under a controlled atmosphere. Solid-state NMR studies were carried out on Bruker DSX 300 MHz and Avance 500 MHz spectrometers. For all experiments, the rotation frequency was set to 10 kHz. Chemical shifts are given with respect to TMS as an external standard, with a precision of 0.2-0.3 and 1 ppm for ¹H and ¹³C NMR, respectively. Parameters used: (i) ¹H MAS NMR spectra, pulse delay, 2 s, 8 - 32 scans per spectrum; (ii) ¹³C CP/MAS NMR spectra, 90° pulse on the protons (pulse length 3.8 μs), then a cross-polarization step with a contact time typically set to 5 ms and finally recording of the ¹³C signal under high-power proton decoupling; pulse delay, 2 s, 20 000 - 100 000 scans per spectrum, an apodization function (exponential) corresponding to a line-broadening of 50 Hz applied to the spectrum. Air-sensitive samples were transferred within a glovebox into a tightly closed zirconia rotor. ESR X-band spectra were recorded on a Bruker X-band spectrometer Elexsys E500 (T=110 K, power 4-16 mW, modulation amplitude 1G), frequency ca. 9.42 GHz). For the correction of magnetic field values, a DPPH standard was used. EasySpin software (Matlab) was used to simulate the EPR spectra.³⁵ For a quantitative evaluation, an integration of the absorbance spectrum was performed and compared to the integration of the spectrum of a vanadyl(IV) sulfate standard. Elemental analyses were performed at the Catalysis Research Institute (IRC, Villeurbanne, France), the Central Analysis Service of the CNRS (Solaize, France) and at LSEO Dijon. Three oxide supports were used, AEROSIL silica from Evonik, silica alumina (25 % alumina, Akzo Nobel), and AEROXIDE ALUC alumina from Evonik were calcined for 24 h at 500 °C under a continuous flow of oxygen and then thermally treated under vacuum (10⁻⁵ mbar) at 500 °C for a minimum of 15 h for a partial dehydroxylation, leading to SiO₂₋₅₀₀, SiO₂-Al₂O₃₋₅₀₀ and Al₂O₃₋₅₀₀, respectively. It was controlled by ESR that the silica, silica-alumina and alumina supports do not show any important paramagnetic impurities such as Fe(III). The BET surface of Al₂O₃₋₅₀₀ is 105 m²/g and the OH density 0.65 mmol/g, corresponding to ca. 3.7 OH/nm².

Reaction of [Ti(CH₂Bu)₄] (TiNp₄) with Different Supports. The impregnation technique consists typically in stirring at 25 °C for 4 h a mixture of the desired support (SiO₂₋₅₀₀, SiO₂-

$\text{Al}_2\text{O}_{3-500}$, $\text{Al}_2\text{O}_{3-500}$, 0.5 - 2.5 g) and a solution of the molecular complex (in excess in comparison to the number of hydroxyl groups of the support) in pentane within a double-Schlenk glass vessel, equipped with a glass frit between its two compartments. After filtration, the solid was kept in the first compartment and washed three times with pentane distilled from the second compartment. All volatile compounds were collected into a large 6 L glass vessel in order to quantify the neopentane evolved during the grafting reaction. The powder was finally dried under vacuum (10^{-5} mmHg) for 4 h, at room temperature, and stored in a glovebox. This protocol allows elimination of the excess of molecular complex, even traces of physisorbed TiNp_4 from the surface and recovery of the gas emitted during the reaction. The Ti contents of the three materials thus obtained, $[\text{TiNp}_x]@\text{SiO}_{2-500}$, $[\text{TiNp}_x]@\text{SiO}_2\text{-Al}_2\text{O}_{3-500}$ and $[\text{TiNp}_x]@\text{Al}_2\text{O}_{3-500}$ were respectively 1.23, 2.25, and 0.79 wt %.

Monitoring the Synthesis of $[\text{Ti}(\text{CH}_2\text{tBu})_x]@\text{Al}_2\text{O}_{3-500}$ and $[\text{Ti-H}]@\text{Al}_2\text{O}_{3-500}$ by *In situ* FTIR. The oxide (25 mg) was pressed into a self-supporting disk, adjusted in the sample holder, and introduced into a cell equipped with CaF_2 windows. The supports were calcined overnight under air at 500 °C and dehydroxylated under vacuum (10^{-5} mbar) at 500 °C. The complex (TiNp_4) was then sublimed under vacuum at 50 °C onto the oxide disk. The solid was then heated at 50 °C for 2 h, and the excess **1** was removed by reverse sublimation at 60 °C and condensed into a tube cooled by liquid nitrogen, which was then sealed off using a blowtorch. An amount of H_2 corresponding to 70 kPa was then introduced into the reactor and the sample heated at 150 °C at a rate of 1 °C/min, maintained at this temperature for 4 h, and then cooled to room temperature. An IR spectrum was recorded at each step.

Hydrogenolysis of Supported Titanium Complex. Typically, the titanium surface organometallic complexes grafted onto dehydroxylated (SiO_{2-500} , $\text{SiO}_2\text{-Al}_2\text{O}_{3-500}$ and $\text{Al}_2\text{O}_{3-500}$) were heated to 150 °C for 2 h in a Schlenk tube under H_2 (550 Torr) first purified on a deoxo/zeolite catalyst. The resulting solids, $[\text{Ti-H}]@\text{SiO}_{2-500}$, $[\text{Ti-H}]@\text{SiO}_2\text{Al}_2\text{O}_{3-500}$ and $[\text{Ti-H}]@\text{Al}_2\text{O}_{3-500}$ were stored in the glovebox. The methane and ethane evolved were further quantified by GC.

Protonolysis of Supported Titanium Hydrides. Protonolysis consisted in the treatment of $[\text{Ti-H}]@\text{SiO}_{2-500}$, $[\text{Ti-H}]@\text{SiO}_2\text{Al}_2\text{O}_{3-500}$ and $[\text{Ti-H}]@\text{Al}_2\text{O}_{3(500)}$ samples with tert-butyl alcohol (40 mbar) for 1 h at 30 °C, followed by the measure of the amount of evolved gases (H_2 , alkanes) by GC. During this treatment, titanium hydrides disappeared while surface $\text{TiO}t\text{Bu}$ species appeared and no modification of the amount of Ti(III) was observed (ESR spectrum recorded less than 24 h after the protonolysis).

Epoxidation of 1-Octene.

In a typical run, the catalyst (*ca.* 10 μmol of titanium, between 20 and 60 mg of supported catalyst) was transferred in a glovebox under an inert atmosphere into a 40 mL Schlenk equipped with a septum for sample removals. 1-Octene (3000 equiv/ mol of Ti) and dodecane (*ca.* 100 mg, the same amount was used for the gas chromatographic standardization) were added *via* syringe under argon into the Schlenk containing the catalyst, which was then fitted with a condenser under argon, a magnetic stirrer and a thermometer. The mixture was stirred and was warmed to 80 °C over 1 h. An anhydrous TBHP solution in pentane (1.5 to 2.0 mmol, 150 - 200 equiv/ mol of Ti) was added dropwise over 2 min *via* a precision syringe. Aliquots were removed at various time intervals and analyzed by gas chromatography.

Hydrogenolysis of a FT Wax. General Procedure.

Mechanical mixtures of supported titanium hydrides (75 μmol of Ti) and wax (400 mg; Aldrich, ASTM D87; mp 70 °C) were charged using a glovebox into a stainless steel cylinder reactor. After connection to the gas lines and purge of the tubes, a flow of hydrogen (20 mL/min), controlled by a mass flow controller (Brooks) under 1 bar of pressure, was sent upward into the catalyst bed, which was heated to 180 °C. Hydrocarbon products were stripped from the liquid medium by the hydrogen flow. Light hydrocarbons were analyzed online by GC (HP 6890 chromatograph equipped with an $\text{Al}_2\text{O}_3/\text{KCl}$ 50 m \times 0.32 mm capillary column and a FID detector for hydrocarbons). Liquid products were condensed at 0 °C and analyzed off-line by GC (HP 5890 chromatograph equipped with an HP5 30 m \times 0.32 mm capillary column and a FID detector).

Polymerization Reaction.

The polymerization reactions were performed in a 100 mL glass-lined stainless steel autoclave, equipped with a magnetic stirrer. The reactor was charged with 50 mg of the supported catalyst (0.79, 1.23, 2.25 wt % Ti on Al_2O_3 -500, SiO_2 -500, and Al_2O_3 - SiO_2 -500, respectively) and 20 mL of dry toluene in the glovebox. The autoclave was connected to a gas line which was flushed with dry ethylene. The reactor was heated to 40 °C and filled with 10 bar of ethylene. The pressure was kept constant for 30 min. The gas and liquid phases were then analyzed in order to check for the presence or absence of oligomers. The reaction was quenched by removing the unreacted ethylene. The polymer was recovered and dried at 50 °C overnight under reduced pressure before the final mass was weighed. High-temperature size exclusion chromatography (HT-SEC) analyses were performed in 1,2,4-trichlorobenzene (TCB) using a Viscotek system (Malvern Instruments) equipped with three columns (PLgel Olexis 300 mm \times 7 mm from

Agilent Technologies) and a refractive index (RI) detector. DSC measurements were performed on a Mettler Toledo DSC 1 apparatus.

Results and Discussion.

1. Grafting of TiNp₄ on Al₂O₃₋₅₀₀.

A Large number of works have been dedicated to elucidate the surface structure of alumina and its interaction with organometallic complexes.³⁶⁻⁴² Alumina is an ionic oxide where the hydroxyl groups are bonded to several different aluminum atoms. Different theoretical models of the surface of alumina have been proposed.^{40,43-45} According to the model reported by Sautet *et al.* five kinds of hydroxyl groups are present on the surface of alumina.⁴⁴ The reactivity of the different aluminum hydroxyl groups depends on the organometallic complex. For instance for isoelectronic complexes of group 3B, Al(*t*Bu)₃ reacts with all kinds of hydroxyl groups,⁴⁶ while Ga(*i*Bu)₃ consumes only part of the available hydroxyl groups.¹⁶ W(\equiv C(*t*Bu))(CH₂*t*Bu)₃ reacts only with tetrahedrally coordinated hydroxyl groups.⁴⁷ On the other hand, Zr(CH₂*t*Bu)₄ can readily react with different hydroxyl groups.⁴⁸ Theoretical investigations have revealed that a protonolysis of a neopentyl ligand in Zr(CH₂*t*Bu)₄ is highly favorable (-201 kJ/mol). Furthermore, the monopodal Zr intermediate species can still undergo a second reaction (having even an activation barrier even lower than that of the first step) with a proximate hydroxyl group to form the bipodal species (-154 kJ/mol). The latter reaction is unfavorable for W(\equiv C(*t*Bu))(CH₂*t*Bu)₃ supported on alumina (100 kJ/mol). Interestingly, for the bipodal Zr species, it has been observed that a neopentyl ligand transfer may occur (practically barrierless, according to DFT calculations) toward a Lewis Al-site and generate a cationic surface species [(Al₅O)₂Zr(CH₂*t*Bu)]⁺ [(Al₅(CH₂*t*Bu)]. The reactivity of Hf(CH₂*t*Bu)₄ on alumina also gives mainly the cationic surface species [(Al₅O)₂Hf(CH₂*t*Bu)]⁺ [(Al₅(CH₂*t*Bu)].^{41,42} In addition, neutral monopodal [(Al₅O)Hf(CH₂*t*Bu)₃] and bipodal [(Al₅O)₂Hf(CH₂*t*Bu)₂] species have also been observed. The difference in reactivity is associated with the steric occupancy of the complex and the size of the transition metal center. Thus, the reactivity of Ti(CH₂*t*Bu)₄ with alumina is expected to be different from the former cases and is further investigated in detail.

1.1. In situ FTIR The reaction of TiNp₄, **1**, with the surface of alumina Al₂O₃₋₅₀₀ partially dehydroxylated and the evolution of the supported titanium complexes under hydrogen is followed by FT-IR (Figure 1). The solid changes color from white for the pure alumina to

become yellow after the grafting reaction. The FTIR data show that the peak at 3777 cm^{-1} characteristic of tetrahedral aluminum hydroxyls ($\text{HO}-\mu_1\text{-Al}_{\text{IV}}$) completely disappears (d in Figure 1). Moreover, the absorption bands around 3726 to 3680 cm^{-1} appear less modified but slightly red shifted to 3672 cm^{-1} , probably due to interactions of hydroxyls with C-H bonds of neopentyl ligands. New bands appear between 2800 and 3000 cm^{-1} , characteristic of CH_3 and CH_2 $\nu_{(\text{C-H})}$ vibrations and from 1229 to 1464 cm^{-1} , $\delta_{(\text{CH}_x)}$ bending vibration bands. They are attributed to Ti neopentyl ligands of grafted surface species (**2a** and **2b** shown in Scheme 1).

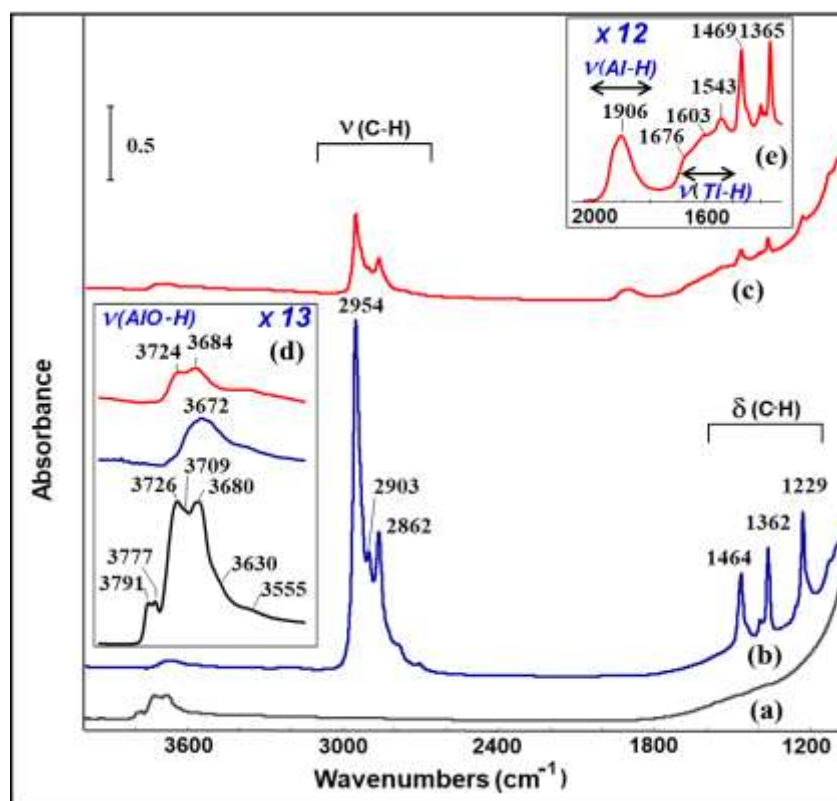
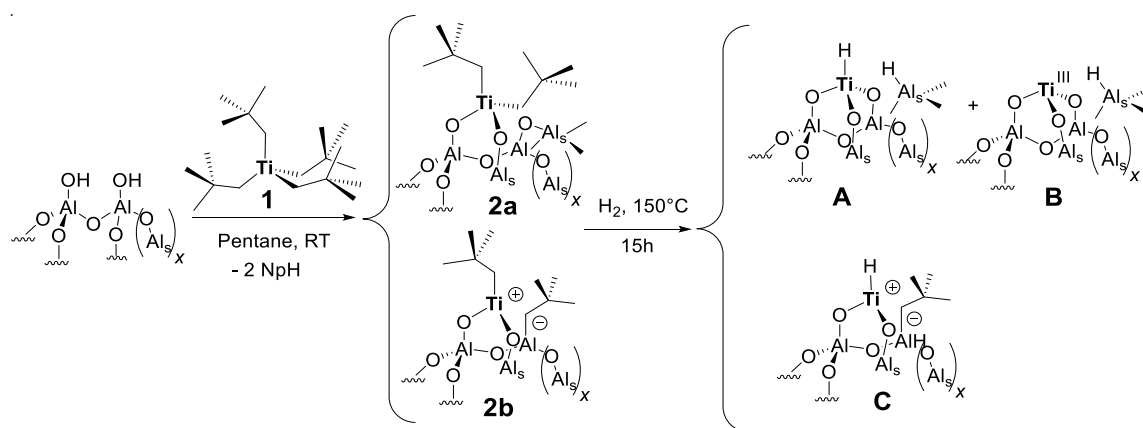


Figure 1. *In situ* FTIR spectra of a) $\text{Al}_2\text{O}_3\text{-500}$, activated at $500\text{ }^\circ\text{C}$ under vacuum overnight; b) after grafting of TiNp_4 on $\text{Al}_2\text{O}_3\text{-500}$; c) after treatment of the resulted supported species by hydrogen for 12 h at $150\text{ }^\circ\text{C}$; d) Enlargement showing the evolution of the $\nu_{(\text{AlO-H})}$ area; e) Enlargement of the $\nu_{(\text{Al-H})}$ and $\nu_{(\text{Ti-H})}$ area, obtained after subtraction of a) to c).

Upon treatment under hydrogen at $150\text{ }^\circ\text{C}$ of the resulting compounds, the intensities of $\nu_{(\text{C-H})}$ and $\delta_{(\text{C-H})}$ vibration bands, attributed to neopentyl groups, strongly decrease but the signals are still present, due to remaining $[\text{Al}_s\text{-Np}]^-$ fragments (see species **2b** and **C** in Scheme 1) as observed in the case of $\text{ZrNp}_x@ \text{Al}_2\text{O}_3\text{-500}$ and $\text{HfNp}_x@ \text{Al}_2\text{O}_3\text{-500}$ supported analogs.^{41,48} In fact, it was observed that a thermal treatment under H_2 at a temperature over $250\text{ }^\circ\text{C}$ is needed to decompose such Al-alkyl fragments.⁴⁶ In addition a band centered at 1906 cm^{-1} is observed (c and e in Figure 1). It is attributed to Al-H stretching vibrations. This component is originated

from a hydride transfer from Ti to Al (**2a** to **A** and **B** in Scheme 1), not from the hydrogenolysis of a transferred neopentyl ligand. Moreover, a broad signal is observed between 1700 and 1500 cm^{-1} (e in Figure 1), apparently composed of three bands at 1676, 1603, 1543 cm^{-1} attributed to stretching vibrations of Ti-H groups, differently coordinated to the surface of alumina. These assignments are further confirmed by H-D exchange experiments and are in agreement with the reactions presented in Scheme 1 that will be described into more details further in the text.



Scheme 1. Grafting reaction of TiNp₄, **1**, onto Al₂O₃₋₅₀₀ leading to neutral, **2a**, and cationic, **2b**, surface species and preparation of alumina supported titanium hydrides, [Ti-H]@Al₂O₃₋₅₀₀, leading to neutral Ti(IV) hydride, **A**, Ti(III), **B**, and Ti(IV) cationic hydride, **C**.

When the supported titanium hydride species are in contact with deuterium gas (1 atm), the intensities of the bands characteristics of a Ti-H stretching mode decreased and shifted, with only slight changes in the shape and intensity of the Al-H band (Figure 2, spectra a to c).

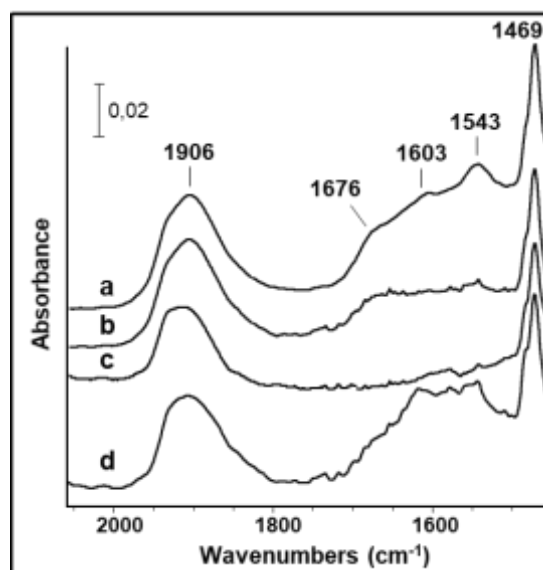


Figure 2. *In situ* FTIR spectra obtained after subtraction of the alumina support contribution: a) [Ti-H]@Al₂O₃₋₅₀₀; b) [Ti-H]@Al₂O₃₋₅₀₀ treated under D₂ for 1h at 25 °C; c) **b** under D₂ overnight; d) reaction of **c** with H₂ for 1h at 150 °C.

The Ti-D vibration band expected around 1150 cm^{-1} was not clearly observed, due to the presence of broad and intense bands characteristic of the alumina framework vibrations. Subsequent reaction with hydrogen reestablished the Ti-H vibrations bands (Figure 2d).

1.2. Mass balance analysis. The grafting of TiNp_4 on $\text{Al}_2\text{O}_{3-500}$ was performed by an impregnation method. 485 mg of TiNp_4 (1.46 mmol) were reacted with 2 g of $\text{Al}_2\text{O}_{3-(500^\circ\text{C})}$ (1.3 mmol of $[\text{Al}_5\text{O-H}]$) in dry pentane for 2 h. Neopentane, $t\text{BuCH}_3$, were detected in the gaseous phase and quantified by gas chromatography (0.69 mmol). After extraction of the excess and a drying at $25\text{ }^\circ\text{C}$ under high vacuum, the amount of carbon and titanium were also measured and gave 1.95 wt% (3.34 mmol) and 0.79 wt % (0.34 mmol) respectively (10 C/Ti on the surface). These results suggest that for each titanium grafted, ca. 2.0 neopentane are released and 2.0 neopentyl groups are left on the material. Thus 0.68 mmol of alumina surface OH groups have reacted (ca. 50 %) with TiNp_4 and the metal surface density for $\text{TiNp}_x@ \text{Al}_2\text{O}_{3-500}$ is ca. 1.0 Ti/nm^2 , as for the grafting ZrNp_4 ⁴⁸ or HfNp_4 ⁴¹ on $\text{Al}_2\text{O}_{3-500}$ supports.

After hydrogenolysis of $\text{TiNp}_x@ \text{Al}_2\text{O}_{3-500}$, methane and ethane were released, their quantification gave $\text{CH}_4/\text{Ti} = 4.7 \pm 0.8$ and $\text{C}_2\text{H}_6/\text{Ti} = 1.7 \pm 0.3$ respectively ($- 8.1\text{ C/Ti}$). The presence of a substantial amount of ethane is due to the fact that Ti can only conduct β -alkyl transfer. Note that according to the mass balance analysis, it remains ca. 2 C/Ti after hydrogenolysis which is due to Al neopentyl fragments obtained after ligand transfer. It further suggests that the grafting of $\text{Ti}(\text{CH}_2t\text{Bu})_4$ on $\text{Al}_2\text{O}_{3-500}$ gives ca. 60% $[(\text{Al}_5\text{O})_2\text{Ti}(\text{CH}_2t\text{Bu})_2]$ (**2a** in Scheme 1) and 40% $[(\text{Al}_5\text{O})_2\text{Ti}(\text{CH}_2t\text{Bu})]^+[(\text{Al}_5(\text{CH}_2t\text{Bu}))^-]$ (**2b** in Scheme 1). The latter distribution is further supported by IR, revealing that it remains ca. 22 % of the $\nu_{(\text{C-H})}$ band intensity, characteristic of residual alkyl groups, after hydrogenolysis (c in Figure 1).

The protonolysis of $[\text{Ti-H}]@ \text{SiO}_{2-500}$ and $[\text{Ti-H}]@ \text{SiO}_2\text{Al}_2\text{O}_{3-500}$ with $t\text{BuOH}$ only led to the emission of dihydrogen ($\text{H}_2/\text{Ti} = 0.85$) and traces of methane, while in the case of $[\text{Ti-H}]@ \text{Al}_2\text{O}_{3(500)}$, neopentane ($\text{NpH}/\text{Ti} = 0.4$) is also evolved with dihydrogen ($\text{H}_2/\text{Ti} = 1.2$) and traces of methane, resulting from the protonolysis of Ti-H, $\text{Al}_5\text{-Np}$ and $\text{Al}_5\text{-H}$ surface species. This neopentane emission agrees in particular with the presence of $[(\text{Al}_5(\text{CH}_2t\text{Bu}))^-]$ surface species which have not reacted with dihydrogen in the conditions of the hydrogenolysis (**2b** and **C** in Scheme 1). $[\text{Ti-H}]@ \text{Al}_2\text{O}_{3-500}$ has then been characterized by NMR and ESR.

1.3. NMR spectroscopy

The solid-state ^1H NMR spectrum of $\text{Ti-Np}_x@Al_2O_{3-500}$ comprises a rather broad resonance centered at 1 ppm which is attributed to methyl and methylene groups of the $\text{Ti-CH}_2\text{C}(\text{CH}_3)_3$ and $\text{Al-CH}_2\text{C}(\text{CH}_3)_3$ fragments and residual $\text{Al}_s\text{-OH}$ sites (Figure S1), while the proton signals of methyl and methylene groups are resolved in the case of $\text{Ti-Np}_x@SiO_{2-500}$ and $\text{Ti-Np}_x@SiO_2-Al_2O_{3-500}$.^{12,32} The complexity of the surface of the alumina support (relative to silica) causes structural diversity in the grafted species, resulting in broadening of the ^1H NMR signals.⁴⁰ The ^{13}C CP-MAS solid state NMR of $\text{TiNp}_x@Al_2O_{3-500}$ is also more complex than those obtained on silica³² and silica-alumina.¹² In order to enhance the signal, a labeled titanium tetrakis-neopentyl organometallic complex was used. It was prepared in five steps from labeled *CO_2 , as already reported elsewhere.^{12,32} On Figure 3, ^{13}C NMR spectra of $[\text{Ti}(\text{CH}_2\text{-}^i\text{Bu})_x]@Al_2O_{3-500}$, and $[\text{Ti}(^*CH_2t\text{Bu})_x]@Al_2O_3$ are shown. Peaks at 31 and 27 ppm are attributed to the methyl groups of the neopentyl coordinated to titanium or aluminum respectively. The signal at 23 ppm is attributed to the methylene groups of $\text{Al-CH}_2\text{C}(\text{CH}_3)_3$ fragments.⁴⁹ Besides, the signals at 103 and 121 ppm (only observed for the labeled sample) are necessarily originated from methylene groups of $\text{Ti-CH}_2\text{C}(\text{CH}_3)_3$ with different environments, including neutral or cationic species (**2a** and **2b** in Scheme 1), as reported in the case of Zr and Hf systems.^{41,48}

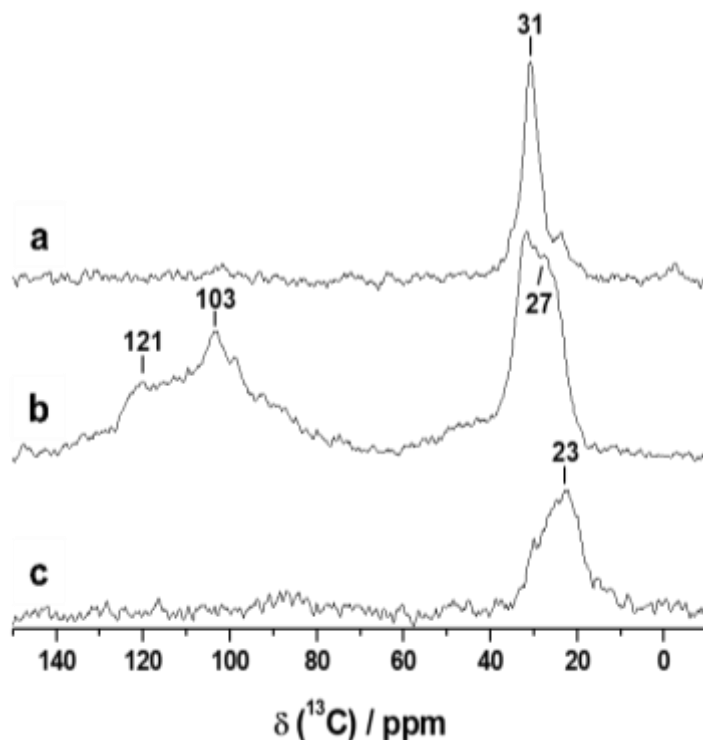


Figure 3. ^{13}C CP-MAS solid-state NMR spectra of **a.** $\text{TiNp}_x@Al_2O_{3-500}$; **b.** ^{13}C enriched $\text{TiNp}_x@Al_2O_{3-500}$ and **c.** $[\text{Ti-H}]@Al_2O_{3-500}$ obtained from the hydrogenolysis of ^{13}C enriched $\text{TiNp}_x@Al_2O_{3-500}$.

After hydrogenolysis, the ^1H NMR spectrum of the sample presents mainly a broad peak, centered at 0.74 ppm attributed to remaining neopentyl groups bound to Al (Figure S1). The broadening of this signal along with the slight shift is due to the presence of Ti(III) paramagnetic species (*vide infra*) in the sample. Due to the more complex nature of sites on the alumina surface and the paramagnetism of $[\text{Ti-H}]\text{@Al}_2\text{O}_{3-500}$, the characteristic Ti-H and Al-H signals, which should both appear in the 3-12 ppm range, are also broadened and very difficult to detect, while for the silica and silica-alumina counterparts, resonances are observed at 4.4 ppm for Si-H and at 8-9 ppm for Ti-H.^{5,12} Besides, the ^{13}C CPMAS spectrum (Figure 3c) features a broad resonance at 23 ppm and corresponds to alkyl groups attached to aluminum,⁴⁹ confirming the occurrence of a neopentyl transfer (leading to $[\text{Np-Als}]^-$ fragments, see species **2b** and **C** in Scheme 1). This type of aluminum alkyl fragment has been already reported to be very stable at 150°C under hydrogen.⁴⁶

1.4. Electron spin resonance (ESR). The nature of the supported titanium complex on $\text{Al}_2\text{O}_{3(500)}$ was further studied by ESR technique (Figure 4).

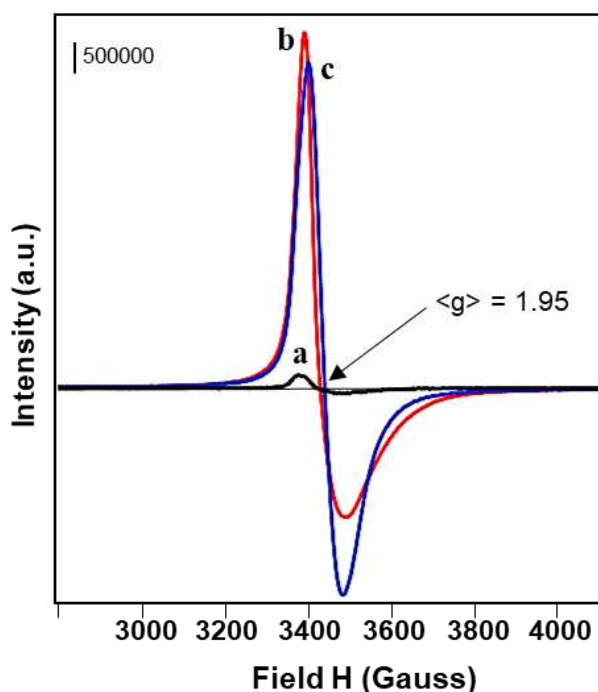


Figure 4: ESR patterns of paramagnetic species on the surface of $\text{Al}_2\text{O}_{3-500}$: a $\text{TiNp}_x\text{@Al}_2\text{O}_{3-500}$ (black); b- $[\text{Ti-H}]\text{@Al}_2\text{O}_{3-500}$ (red); c- after the butanolysis of $[\text{Ti-H}]\text{@Al}_2\text{O}_{3-500}$ (blue).

The ESR signal of TiNp_4 on alumina shows an overall width of ca. 800 G and an average ESR g-factor: $g_{\text{av}} = 1.95$ (Figure 4). It is consistent with an unpaired electron in a metal based orbital typical of a Ti(III) radical.⁵⁰ From the double integration of the signal, compared to the

integration of the spectrum of a vanadyl sulfate standard, only a small fraction of Ti(III) is present in this sample, (ca. 1 % of the total amount of supported Ti). After hydrogenolysis, the signal observed (Figure 4b) is much more intense and its integration indicates that ca. 30% of the supported titanium is Ti(III). After the protonolysis of [Ti-H]@Al₂O₃₋₅₀₀ with *t*BuOH, the shape of the signal has changed and is more symmetric (c in Figure 4), probably due to a coordination of *t*BuOH on the Ti(III) sites as a L-type ligand. Moreover the intensity of the signal is not much affected (ca. 28% of the supported Ti is Ti(III)), showing that in these conditions *t*BuOH did not react with Ti(III).

After the hydrogenolysis of (Al₅O)₂TiNp₂, **2a**, and [(Al₅O)₂TiNp]⁺ [Np-Al₅], **2b**, the resulting material, [Ti-H]@Al₂O₃₋₅₀₀, is composed of different surface species (see **A**, **B** and **C** in Scheme 1): Neutral tripodal hydrides, [(Al₅O)₃Ti-H] (**A**, ca. 30 %), formed concomitantly with Al₅-H surface fragments; Ti(III) radicals, [(Al₅O)₃Ti(III)] (**B**, ca. 30 %) and bipodal cationic hydrides, [(Al₅O)₂Ti-H]⁺ [Np-Al₅] (**C**, ca. 40 %). This repartition was deduced from the results of mass balance analysis, protonolysis with *t*BuOH (NpH emission for **C**) and EPR (Ti(III) proportion for **B**). It also agrees with the IR and NMR studies. These species will lead to different catalytic reactivities. Their proportions are summarized in Table 1. It should be noticed that the cationic species, **C**, only exist for the alumina support and the Ti(III) proportion is ca. twice more important on alumina than on silica or silica-alumina supports.

Table 1. Proportion of the different supported species in the different Ti-H@oxide materials.

	A *	B *	C *
[Ti-H]@Al ₂ O ₃₋₅₀₀	30 %	30 %	40 %
[Ti-H]@SiO ₂ -Al ₂ O ₃₋₅₀₀ ¹²	85 %	15 %	0
[Ti-H]@SiO ₂ ⁵	85 %	15 %	0

*Structures of species **A**, **B** and **C** are presented above, in Scheme 1. The relative error on each figure is ± 15 % (e. g. for **C** on Al₂O₃₋₅₀₀, the proportion is 40 ± 6 %)

2. Catalytic performances.

In this part of the study, the catalytic activities of titanium hydrides supported on different oxides (silica, silica-alumina, alumina), materials noted [Ti-H]@SiO₂, [Ti-H]@SiO₂-Al₂O₃ and [Ti-H]@Al₂O₃ were investigated as polyfunctional catalysts in three different reactions: the

epoxidation of 1-octene to 1,2-epoxyoctane,⁵¹ the low temperature hydrogenolysis of a FT-wax¹² and the polymerization of ethylene.⁵² These studies provide a direct comparison of the support effect in the chosen reactions.

2.1. 1-octene epoxidation. The catalytic performances for the epoxidation of 1-octene by *tert*-butyl hydroperoxide (Scheme S1) of these well-defined titanium hydride grafted species were evaluated. A blank test with bare alumina showed no significant epoxidation reaction at 80 °C and that a slow TBHP degradation occurred:⁵³ 6 % in 1 h; 12 % in 4 h. The formation of 1,2-epoxyoctane and the TBHP consumption with time are represented in Figure 5.

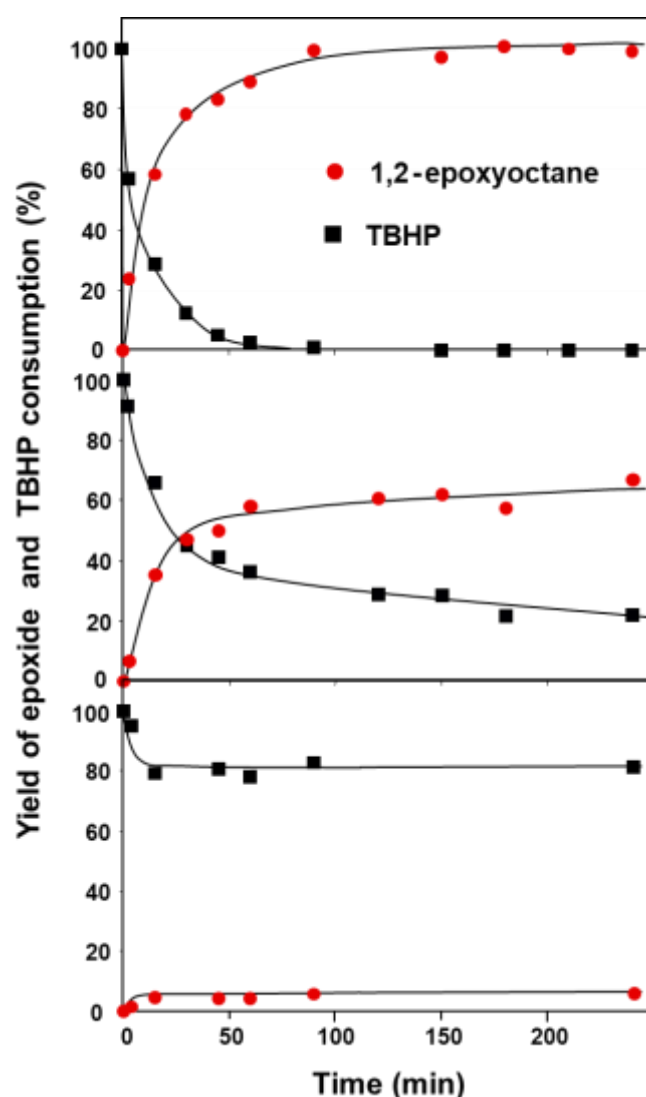


Figure 5: Activity of supported [Ti-H] species for 1-octene epoxidation by TBHP: yield of 1,2-epoxyoctane and conversion of TBHP a) [Ti-H]@SiO₂-500; b) [Ti-H]@SiO₂-Al₂O₃-500; c) [[Ti-H]@Al₂O₃-500.

The initial activities, determined after less than 4 minutes and the turn over frequency (TOF) obtained after fifteen minutes of reaction for the titanium hydrides supported on the three supports, silica, silica-alumina and alumina are summarized in Table 2.

The conversion of TBHP versus time showed that the reaction is faster in the presence of the catalyst supported onto silica than onto silica-alumina; indeed, after 60 min the yield of 1,2-epoxyoctane is more than 90%, while it is about 60% for Ti-H@SiO₂-Al₂O₃₋₅₀₀ and it is only 5% for [Ti-H]@Al₂O₃₋₅₀₀ (Figure 5). The catalyst resulting from [Ti-H]@SiO₂₋₅₀₀ is then the most active and stable.

Table 2. Initial activities and TOF after 15 min of reaction for the epoxidation of 1-octene by TBHP.

	Initial activity (h ⁻¹)	TOF (h ⁻¹) after 15 min
[Ti-H]@SiO ₂	1050	465
[Ti-H]@SiO ₂ -Al ₂ O ₃	310	210
[Ti-H]@Al ₂ O ₃	34	28

This catalytic reaction should first involve a protonolysis of Ti-H moieties by TBHP along with the formation of hydrogen and a Ti-OO*t*Bu active surface species (Scheme S2). The formation of the epoxide consists in an oxygen transfer to the olefin, as already reported in the literature.⁵⁴⁻⁵⁶ Ti(III) (species C) may also catalyze an epoxidation with TBHP,⁵⁷ but the reaction rate is reported to be rather low, even for an allylic alcohol.

The results suggest that the support plays a central role in the stability of the catalyst. In the case of the alumina support, the limited activity seems due to a poisoning of the catalytic site, most likely by strongly coordinated chelating ligands as β-methoxy-alcohols and diols. It is known that the most electrophilic Lewis acid sites can catalyze the opening of an epoxide at moderated temperatures.⁵⁸⁻⁶¹ On the alumina support, the most electrophilic cationic C type Ti sites may play this role, thus producing β-alkoxy alcohols chelating ligands strongly adsorbed on Ti sites that would lead to a deactivation of the catalyst. On another hand, the presence of water or resulting ≡Ti-OH groups has been proposed for the ring opening of epoxides and the formation of diols that tend to deactivate the catalyst.⁶²⁻⁶⁴ The formation of water may come from the reaction of *t*BuOH or TBHP with residual Al_sOH groups of alumina to form Al_s-OR or Al_s-OOR surface species. Besides pure alumina itself is known to also catalyze the epoxide

opening with alcohols or water into β -alkoxy-alcohols and diols.^{65,66} However an alcohol dehydration on alumina would occur at higher temperatures.^{67,68} Current findings suggest that aluminum-free supports are preferable in this type of epoxidation reaction.

2.2. FT wax hydrogenolysis. The catalytic performances of the three supported titanium hydrides, materials, noted $[\text{Ti-H}]\text{@SiO}_2\text{-500}$, $[\text{Ti-H}]\text{@SiO}_2\text{-Al}_2\text{O}_3\text{-500}$ and $[\text{Ti-H}]\text{@Al}_2\text{O}_3\text{-500}$ were evaluated in the hydrogenolysis of paraffin waxes, an important reaction in petrochemistry. The effect of the support itself, in the absence of the titanium hydrides was studied and the conversions were found to be negligible for the three oxides. The evolution of the gaseous phase was followed by gas chromatography, in particular for the (C1-C4) gas cut (Figure S2). The liquids were recovered in a specific compartment and characterized. The reaction was considered as over when no more gas was detected by GC. In fact the end of the reaction was observed for $[\text{Ti-H}]\text{@SiO}_2\text{-Al}_2\text{O}_3$ and $[\text{Ti-H}]\text{@Al}_2\text{O}_3$ after 14 and 10 h respectively (no more wax in the reactor), while for $[\text{Ti-H}]\text{@SiO}_2\text{-500}$, the reaction was stopped, for a wax conversion of only 30 %, after 26 h.

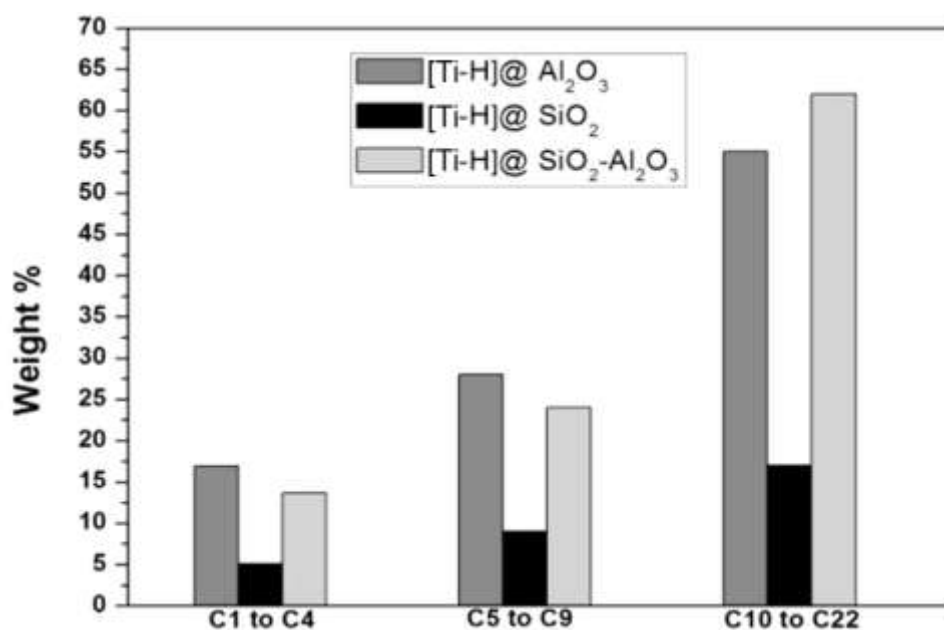


Figure 6: Yields in the three fractions, gas, gasoline, and diesel during the hydrogenolysis of a FT wax.

The products of hydrogenolysis have been divided into three fractions, gas (C₁-C₄), gasoline (C₅-C₉) and diesel (C₁₀-C₂₂) cuts. The yields of the different fractions are highlighted in Figure 6. As shown, the titanium supported on silica is less active and the reaction was not completed

even after 26 h, while for the two other supports it was completed. In the case of alumina, slightly higher amounts of gas and gasoline were obtained compared to the silica-alumina support whereas the diesel fraction was slightly more dominant in the presence of silica-alumina than alumina. The amounts of each compound before and after the hydrogenolysis reaction are highlighted in Figure S3.

While the same amount of Ti is used, the reaction rate is lower for [Ti-H]@SiO₂₋₅₀₀, as it can be observed for low reaction times for C1-C4 gases production (Figure S2). The mechanism proposed for such hydrogenolysis reactions catalyzed by group 4 metals is based on a C-H bond activation in the paraffinic chain by the metal hydride in a d⁰ configuration through a σ -bond metathesis, with the formation of a metal-alkyl complex and liberation of dihydrogen. Then a β -alkyl transfer step, leading to the C-C bond cleavage with the formation of a new metal-alkyl complex and an olefin with a smaller carbon chain, would be the rate-limiting step, thermodynamically unfavorable.^{69,70} The following hydrogenation of the olefinic double bond would provide the driving force to make the process run. The proximity of a Lewis acid centre and a stronger electrophilicity of the metal site would then facilitate the key β -alkyl transfer step of the proposed mechanism through the weakening of a C β -alkyl bond by an additional alkyl-Lewis acid interaction and the formation of a more stable Ti-olefin π -complex. This may explain the higher activity observed for [Ti-H]@SiO₂-Al₂O₃₋₅₀₀ and [Ti-H]@Al₂O₃₋₅₀₀ compared to [Ti-H]@SiO₂₋₅₀₀.

2.3. Ethylene polymerization. The activities of the supported hydrides toward ethylene polymerization were also studied. The supported hydrides showed interesting activities at 40 °C under 10 bar of ethylene without any co-catalyst (Table 3). The titanium hydrides supported onto alumina have an activity of 915 g.mmol⁻¹.h⁻¹ which is more than three times higher than for the ones supported onto silica or silica-alumina. Titanium hydrides supported onto silica are slightly more active than the one supported onto silica-alumina (270 vs 220 g.mmol⁻¹.h⁻¹).

In our protocol, the mass of catalyst is the same but the Ti amount is different and differently distributed among the three categories of surface sites (A, B or C, see Scheme 1 and Table 1): 13 μ mol Ti for [Ti-H]@SiO₂₋₅₀₀ (A: 11 μ mol, B: 2 μ mol, C: 0); 24 μ mol Ti for [Ti-H]@SiO₂-Al₂O₃₋₅₀₀ (A: 20 μ mol, B: 4 μ mol, C: 0); 8.3 μ mol Ti for [Ti-H]@Al₂O₃₋₅₀₀ (A: 2.5 μ mol, B: 2.5 μ mol, C: 3.3 μ mol). From these results it can be deduced that the cationic species, C, is more active than Ti(IV) neutral species, A and that increasing fractions of B and C sites are correlated with increasing yields.

Table 3: Results obtained for ethylene polymerization over [Ti-H] species supported onto different oxides: [Ti-H]@SiO₂₋₅₀₀, [Ti-H]@SiO₂-Al₂O₃₋₅₀₀ and [Ti-H]@Al₂O₃₋₅₀₀.^a

Catalyst	Ti (wt %)	Amount of PE (g)	Activity (g.mmol _{Ti} ⁻¹ .h ⁻¹)	M _n ^b (10 ³ g/mol)	PDI (M _w /M _n)	T _m ^c
[Ti-H]@SiO ₂₋₅₀₀	1.23	1.75	270	156	1.98	134
[Ti-H]@SiO ₂ -Al ₂ O ₃₋₅₀₀	2.25	2.57	220	195	1.92	135
[Ti-H]@Al ₂ O ₃₋₅₀₀	0.79	3.77	915	195	1.78	136

^a Experimental conditions: T = 40 °C, P = 10 bar, t = 30 min, V = 20 mL toluene, Catalyst: 50 mg; ^b From GPC; ^c From DSC.

The mechanism of polymerization involves an insertion of ethylene in the Ti-H bond, followed by the insertion of ethylene into a Ti-alkyl bond, a propagation step, on preferably highly electron deficient center, in particular cationic species. Importantly, cationic Ti-H type species as C are unknown in homogeneous catalysis, due to a rapid deactivation through the formation of inactive dimeric species. This latter deactivation scheme can be avoided with firmly anchored supported species.

Conclusion.

Titanium hydrides supported onto three different oxides (silica, silica-alumina, and alumina) were successfully prepared via the surface organometallic chemistry approach. [Ti-H]@Al₂O₃₋₅₀₀ is reported for the first time and has been extensively characterized by IR, solid state NMR, mass balance analysis and ESR. Their activities in three different reactions (epoxidation of 1-octene, depolymerization of a FT-wax and polymerization of ethylene) were studied. The material prepared with this strategy have led to heterogeneous catalysts operating under relatively mild conditions. This work demonstrates that the activity and the selectivity of the catalysts are in relation with the support. In the case of the epoxidation reaction of 1-octene, it was shown that the presence of aluminum (SiO₂-Al₂O₃₋₅₀₀ and Al₂O₃₋₅₀₀ supports) inhibited the reaction, due to the presence of Lewis and strong Bronsted acid sites that can produce chelate poisoning molecules such as diols. The effect of support on the hydrogenolysis of FT-waxes was examined and [Ti-H]@Al₂O₃₋₅₀₀ exhibited the highest activity with an important diesel selectivity, slightly higher than the one of [Ti-H]@SiO₂-Al₂O₃₋₅₀₀. Conversely, [Ti-H]@SiO₂₋₅₀₀ was much less active, which was attributed to a lower electrophilicity of Ti active centers

and the lack of acid sites surrounding the Ti-H active site. The three different catalysts showed to be active in ethylene polymerization without any addition of co-catalyst. However, the alumina supported sample offered a more significant amount of cationic Ti propagation sites and boosted the polymerization activity. This study showed that a proper choice of the support may strongly alter the catalytic properties for supported Ti-H species, due to the presence of neutral and/or cationic supported Ti-H species.

Acknowledgements.

The authors wish to thank CNRS, the French Ministry of Higher Education and Research and CPE-Lyon for financial support.

Supporting Information.

^1H NMR spectra of $[\text{TiNp}_x]@\text{Al}_2\text{O}_{3-500}$ and $[\text{Ti-H}]@\text{Al}_2\text{O}_{3-500}$; Schemes presenting the epoxidation reaction and a proposed mechanism; Figures showing the evolution of cumulated C1-C4 gas products during the hydrogenolysis of a FT-wax catalyzed by the three catalysts and the whole products distributions before and after the reaction

AUTHOR INFORMATION

Corresponding Authors

* e-mail for A.D.M.: aimery.de-mallmann@univ-lyon1.fr

* e-mail for M.T.: mostafa.taoufik@univ-lyon1.fr

* e-mail for L.C.: cherif.larabi@univ-lyon1.fr

Author Contributions

The manuscript was written through contributions of all authors. All authors have given approval to the final version of the manuscript.

Notes

The authors declare no competing financial interest.

References.

- (1) Song, J.-R.; Wen, L.-X.; Shao, L.; Chen, J.-F. Preparation and Characterization of Novel Pd/SiO₂ and Ca-Pd/SiO₂ Egg-Shell Catalysts with Porous Hollow Silica. *Appl. Surf. Sci.* **2006**, *253* (5), 2678–2684. <https://doi.org/10.1016/j.apsusc.2006.05.035>.
- (2) Martha Barroso-Quiroga, M.; Eduardo Castro-Luna, A. Catalytic Activity and Effect of Modifiers on Ni-Based Catalysts for the Dry Reforming of Methane. *Int. J. Hydrog. Energy* **2010**, *35* (11, SI), 6052–6056. <https://doi.org/10.1016/j.ijhydene.2009.12.073>.
- (3) Ramaswamy, V.; Malwadkar, S.; Chilukuri, S. Cu-Ce Mixed Oxides Supported on Al-Pillared Clay: Effect of Method of Preparation on Catalytic Activity in the Preferential Oxidation of Carbon Monoxide. *Appl. Catal. B* **2008**, *84* (1–2), 21–29. <https://doi.org/10.1016/j.apcatb.2008.02.023>.
- (4) Long, J.; Wang, X.; Zhang, G.; Dong, J.; Yan, T.; Li, Z.; Fu, X. A Mononuclear Cyclopentadiene-Iron Complex Grafted in the Supercages of HY Zeolite: Synthesis, Structure, and Reactivity. *Chem. Eur. J.* **2007**, *13* (28), 7890–7899. <https://doi.org/10.1002/chem.200700505>.
- (5) Basset, J.-M.; Psaro, R.; Roberto, D. *Modern Surface Organometallic Chemistry*; Wiley-VCH Verlag GmbH & Co: Weinheim, 2009.
- (6) Samantaray, M. K.; D'Eia, V.; Pump, E.; Falivene, L.; Harb, M.; Chikh, S. O.; Cavallo, L.; Basset, J.-M. The Comparison between Single Atom Catalysis and Surface Organometallic Catalysis. *Chem. Rev.* **2020**, *120* (2), 734–813. <https://doi.org/10.1021/acs.chemrev.9b00238>.
- (7) Popoff, N.; Mazoyer, E.; Pelletier, J.; Gauvin, R. M.; Taoufik, M. Expanding the Scope of Metathesis: A Survey of Polyfunctional, Single-Site Supported Tungsten Systems for Hydrocarbon Valorization. *Chem. Soc. Rev.* **2013**, *42* (23), 9035–9054. <https://doi.org/10.1039/c3cs60115c>.
- (8) Larabi, C.; Merle, N.; Le Quemener, F.; Rouge, P.; Berrier, E.; Gauvin, R. M.; Le Roux, E.; de Mallmann, A.; Szeto, K. C.; Taoufik, M. New Synthetic Approach towards Well-Defined Silica Supported Tungsten Bisoxo, Active Catalysts for Olefin Metathesis. *Catal. Commun.* **2018**, *108*, 51–54. <https://doi.org/10.1016/j.catcom.2018.01.031>.
- (9) Larabi, C.; Szeto, K. C.; Bouhoute, Y.; Charlin, M. O.; Merle, N.; De Mallmann, A.; Gauvin, R. M.; Delevoye, L.; Taoufik, M. Solvent-Free Ring-Opening Metathesis Polymerization of Norbornene over Silica-Supported Tungsten-Oxo Perhydrocarbyl Catalysts. *Macromol. Rapid Commun.* **2016**, *37* (22), 1832–1836. <https://doi.org/10.1002/marc.201600419>.
- (10) Barman, S.; Merle, N.; Minenkov, Y.; De Mallmann, A.; Samantaray, M. K.; Le Quemener, F.; Szeto, K. C.; Abou-Hamad, E.; Cavallo, L.; Taoufik, M.; Basset, J.-M. Well-Defined Silica Grafted Molybdenum Bis(Imido) Catalysts for Imine Metathesis Reactions. *Organometallics* **2017**, *36* (8), 1550–1556. <https://doi.org/10.1021/acs.organomet.7b00115>.
- (11) Norsic, S.; Larabi, C.; Delgado, M.; Garron, A.; de Mallmann, A.; Santini, C.; Szeto, K. C.; Basset, J.-M.; Taoufik, M. Low Temperature Hydrogenolysis of Waxes to Diesel Range Gasoline and Light Alkanes: Comparison of Catalytic Properties of Group 4, 5 and 6 Metal Hydrides Supported on Silica-Alumina. *Catal. Sci. Technol.* **2012**, *2* (1), 215–219. <https://doi.org/10.1039/c1cy00256b>.
- (12) Larabi, C.; Merle, N.; Norsic, S.; Taoufik, M.; Baudouin, A.; Lucas, C.; Thivolle-Cazat, J.; de Mallmann, A.; Basset, J.-M. Surface Organometallic Chemistry of Titanium on Silica-Alumina and Catalytic Hydrogenolysis of Waxes at Low

- Temperature. *Organometallics* **2009**, *28* (19), 5647–5655.
<https://doi.org/10.1021/om900151a>.
- (13) Soulivong, D.; Norsic, S.; Taoufik, M.; Coperet, C.; Thivolle-Cazat, J.; Chakka, S.; Basset, J.-M. Non-Oxidative Coupling Reaction of Methane to Ethane and Hydrogen Catalyzed by the Silica-Supported Tantalum Hydride: (SiO)₂Ta-H. *J. Am. Chem. Soc.* **2008**, *130* (15), 5044–5045. <https://doi.org/10.1021/ja800863x>.
- (14) Szeto, K. C.; Norsic, S.; Hardou, L.; Le Roux, E.; Chakka, S.; Thivolle-Cazat, J.; Baudouin, A.; Papaioannou, C.; Basset, J.-M.; Taoufik, M. Non-Oxidative Coupling of Methane Catalysed by Supported Tungsten Hydride onto Alumina and Silica-Alumina in Classical and H-2 Permeable Membrane Fixed-Bed Reactors. *Chem. Commun.* **2010**, *46* (22), 3985–3987. <https://doi.org/10.1039/c0cc00007h>.
- (15) Szeto, K. C.; Loges, B.; Merle, N.; Popoff, N.; Quadrelli, E. A.; Jia, H.; Berrier, E.; De Mallmann, A.; Deleyoye, L.; Gauvin, R. M.; Taoufik, M. Vanadium Oxo Organometallic Species Supported on Silica for the Selective Non-Oxidative Dehydrogenation of Propane. *Organometallics* **2013**, *32* (21), 6452–6460.
<https://doi.org/10.1021/om400795s>.
- (16) Szeto, K. C.; Jones, Z. R.; Merle, N.; Rios, C.; Gallo, A.; Le Quemener, F.; Deleyoye, L.; Gauvin, R. M.; Scott, S. L.; Taoufik, M. A Strong Support Effect in Selective Propane Dehydrogenation Catalyzed by Ga(i-Bu)₃ Grafted onto Gamma-Alumina and Silica. *ACS Catal.* **2018**, *8* (8), 7566–7577.
<https://doi.org/10.1021/acscatal.8b00936>.
- (17) Szeto, K. C.; Gallo, A.; Hernandez-Morejudo, S.; Olsbye, U.; De Mallmann, A.; Lefebvre, F.; Gauvin, R. M.; Deveyoye, L.; Scott, S. L.; Taoufik, M. Selective Grafting of Ga(i-Bu)₃ on the Silanols of Mesoporous H-ZSM-5 by Surface Organometallic Chemistry. *J. Phys. Chem. C* **2015**, *119* (47), 26611–26619.
<https://doi.org/10.1021/acs.jpcc.5b09289>.
- (18) Al Maksoud, W.; Gevers, L. E.; Vittenet, J.; Outd-Chikh, S.; Telalovic, S.; Bhatte, K.; Abou-Hamad, E.; Anjum, D. H.; Hedhili, M. N.; Vishwanath, V.; Alhazmi, A.; Atmusaiteer, K.; Basset, J. M. A Strategy to Convert Propane to Aromatics (BTX) Using TiNp₄ Grafted at the Periphery of ZSM-5 by Surface Organometallic Chemistry. *Dalton Trans.* **2019**, *48* (19), 6611–6620. <https://doi.org/10.1039/c9dt00905a>.
- (19) Szeto, K. C.; Merle, N.; Rios, C.; Rouge, P.; Castelbou, J. L.; Taoufik, M. Tailoring the Selectivity in 2-Butene Conversion over Supported d(0) Group 4, 5 and 6 Metal Hydrides: From Dimerization to Metathesis. *Catal. Sci. Technol.* **2015**, *5* (10), 4765–4771. <https://doi.org/10.1039/c5cy00582e>.
- (20) Meunier, D.; Piechaczyk, A.; de Mallmann, A.; Basset, J. Silica-Supported Tantalum Catalysts for Asymmetric Epoxidations of Allyl Alcohols. *Angew. Chem. Int. Ed.* **1999**, *38* (23), 3540–3542. [https://doi.org/10.1002/\(SICI\)1521-3773\(19991203\)38:23<3540::AID-ANIE3540>3.0.CO;2-U](https://doi.org/10.1002/(SICI)1521-3773(19991203)38:23<3540::AID-ANIE3540>3.0.CO;2-U).
- (21) Basset, J.-M.; Coperet, C.; Soulivong, D.; Taoufik, M.; Cazat, J. T. Metathesis of Alkanes and Related Reactions. *Acc. Chem. Res.* **2010**, *43* (2), 323–334.
<https://doi.org/10.1021/ar900203a>.
- (22) Taoufik, M.; Le Roux, E.; Thivolle-Cazat, J.; Basset, J.-M. Direct Transformation of Ethylene into Propylene Catalyzed by a Tungsten Hydride Supported on Alumina: Trifunctional Single-Site Catalysis. *Angew. Chem. Int. Ed.* **2007**, *46* (38), 7202–7205.
<https://doi.org/10.1002/anie.200701199>.
- (23) Le Quemener, F.; Barman, S.; Merle, N.; Aljuhani, M. A.; Samantaray, M. K.; Saih, Y.; Szeto, K. C.; De Mallmann, A.; Minenkov, Y.; Huang, K.-W.; Cavallo, L.; Taoufik, M.; Basset, J.-M. Metathetic Oxidation of 2-Butenes to Acetaldehyde by Molecular

- Oxygen Using the Single-Site Olefin Metathesis Catalyst (SiO)₂Mo(=O)₂. *ACS Catal.* **2018**, 8 (8), 7549–7555. <https://doi.org/10.1021/acscatal.8b01767>.
- (24) Samantaray, M. K.; Pump, E.; Bendjeriou-Sedjerari, A.; D'Elia, V.; Pelletier, J. D. A.; Guidotti, M.; Psaro, R.; Basset, J.-M. Surface Organometallic Chemistry in Heterogeneous Catalysis. *Chem. Soc. Rev.* **2018**, 47 (22), 8403–8437. <https://doi.org/10.1039/c8cs00356d>.
- (25) Clerici, M.; Bellussi, G.; Romano, U. Synthesis of Propylene-Oxide from Propylene and Hydrogen-Peroxide Catalyzed by Titanium Silicalite. *J. Catal.* **1991**, 129 (1), 159–167. [https://doi.org/10.1016/0021-9517\(91\)90019-Z](https://doi.org/10.1016/0021-9517(91)90019-Z).
- (26) Buijink, J.; van Vlaanderen, J.; Crocker, A.; Niele, E. Propylene Epoxidation over Titanium-on-Silica Catalyst - the Heart of the SMPO Process. *Catal. Today* **2004**, 93–5, 199–204. <https://doi.org/10.1016/j.cattod.2004.06.041>.
- (27) Aldrich, K. E.; Odom, A. L. Titanium-Catalyzed Hydroamination and Multicomponent Coupling with a Simple Silica-Supported Catalyst. *Organometallics* **2018**, 37 (23), 4341–4349. <https://doi.org/10.1021/acs.organomet.8b00313>.
- (28) Zhizhko, P. A.; Pichugov, A. V.; Bushkov, N. S.; Rumyantsev, A. V.; Utegenov, K. I.; Talanova, V. N.; Strelkova, T. V.; Lebedev, D.; Mance, D.; Zarubin, D. N. Catalytic Imido-Transfer Reactions of Well-Defined Silica-Supported Titanium Imido Complexes Prepared via Surface Organometallic Chemistry. *Organometallics* **2020**, 39 (7), 1014–1023.
- (29) Popoff, N.; Espinas, J.; Pelletier, J.; Macqueron, B.; Szeto, K. C.; Boyron, O.; Boisson, C.; Del Rosal, I.; Maron, L.; De Mallmann, A.; Gauvin, R. M.; Taoufik, M. Small Changes Have Consequences: Lessons from Tetrabenzyltitanium and -Zirconium Surface Organometallic Chemistry. *Chem. Eur. J* **2013**, 19 (3), 964–973. <https://doi.org/10.1002/chem.201202737>.
- (30) Rosier, C.; Niccolai, G.; Basset, J. Catalytic Hydrogenolysis and Isomerization of Light Alkanes over the Silica-Supported Titanium Hydride Complex (SiO)₃TiH. *J. Am. Chem. Soc.* **1997**, 119 (50), 12408–12409. <https://doi.org/10.1021/ja972488i>.
- (31) Alladin, T.; Beaudoin, M.; Scott, S. Thermolysis of Silica-Supported Bis(Neopentyl) Complexes of Titanium and Zirconium. *Inorg. Chim. Acta* **2003**, 345, 292–298. [https://doi.org/10.1016/S0020-1693\(02\)01272-0](https://doi.org/10.1016/S0020-1693(02)01272-0).
- (32) Bini, F.; Rosier, C.; Saint-Arroman, R. P.; Neumann, E.; Dablemont, C.; de Mallmann, A.; Lefebvre, F.; Niccolai, G. P.; Basset, J.-M.; Crocker, M.; Buijink, J.-K. Surface Organometallic Chemistry of Titanium: Synthesis, Characterization, and Reactivity of (Si-O)_nTi(CH₂C(CH₃)₃)_{4-n} (n = 1, 2) Grafted on Aerosil Silica and MCM-41. *Organometallics* **2006**, 25 (15), 3743–3760. <https://doi.org/10.1021/om050675g>.
- (33) Cheon, J.; Rogers, D.; Girolami, G. Mechanistic Studies of the Thermolysis of Tetraneopentyltitanium(IV) .1. Solution Evidence That Titanium Alkylidenes Activate Saturated Hydrocarbons. *J. Am. Chem. Soc.* **1997**, 119 (29), 6804–6813. <https://doi.org/10.1021/ja970811b>.
- (34) Gao, Y.; Hanson, R.; Klunder, J.; Ko, S.; Masamune, H.; Sharpless, K. Catalytic Asymmetric Epoxidation and Kinetic Resolution-Modified Procedures Including In situ Derivatization. *J. Am. Chem. Soc.* **1987**, 109 (19), 5765–5780. <https://doi.org/10.1021/ja00253a032>.
- (35) Stoll, S.; Schweiger, A. EasySpin, a Comprehensive Software Package for Spectral Simulation and Analysis in EPR. *J. Magn. Res.* **2006**, 178 (1), 42–55. <https://doi.org/10.1016/j.jmr.2005.08.013>.
- (36) Joubert, J.; Delbecq, F.; Sautet, P. Alkane Metathesis by a Tungsten Carbyne Complex Grafted on Gamma Alumina: Is There a Direct Chemical Role of the Support? *J. Catal.* **2007**, 251 (2), 507–513. <https://doi.org/10.1016/j.jcat.2007.07.035>.

- (37) Joubert, J.; Delbecq, F.; Thieuleux, C.; Taoufik, M.; Blanc, F.; Coperet, C.; Thivolle-Cazat, J.; Basset, J.-M.; Sautet, P. Synthesis, Characterization, and Catalytic Properties of Gamma-Al₂O₃-Supported Zirconium Hydrides through a Combined Use of Surface Organometallic Chemistry and Periodic Calculations. *Organometallics* **2007**, *26* (14), 3329–3335. <https://doi.org/10.1021/om070145f>.
- (38) Szeto, K. C.; Merle, N.; Trebosc, J.; Taoufik, M.; Gauvin, R. M.; Pourpoint, F.; Delevoye, L. Caveat on the Actual Robustness of Heteronuclear NMR Methods for Probing the Surface of Gamma-Alumina and Related Catalysts. *J. Phys. Chem. C* **2019**, *123* (20), 12919–12927. <https://doi.org/10.1021/acs.jpcc.9b02634>.
- (39) Knözinger, H.; Ratnasamy, P. Catalytic Aluminas - Surface Models and Characterization of Surface Sites. *Catal. Rev. Sci. Eng.* **1978**, *17* (1), 31–70. <https://doi.org/10.1080/03602457808080878>.
- (40) Taoufik, M.; Szeto, K. C.; Merle, N.; Del Rosal, I.; Maron, L.; Trebosc, J.; Tricot, G.; Gauvin, R. M.; Delevoye, L. Heteronuclear NMR Spectroscopy as a Surface-Selective Technique: A Unique Look at the Hydroxyl Groups of Gamma-Alumina. *Chem. Eur. J* **2014**, *20* (14), 4038–4046. <https://doi.org/10.1002/chem.201304883>.
- (41) Delgado, M.; Santini, C. C.; Elbecq, F.; Wischert, R.; Le Guennic, B.; Tosin, G.; Spitz, R.; Basset, J.-M.; Sautet, P. Alumina as a Simultaneous Support and Co Catalyst: Cationic Hafnium Complex Evidenced by Experimental and DFT Analyses. *J. Phys. Chem. C* **2010**, *114* (43), 18516–18528. <https://doi.org/10.1021/jp104999n>.
- (42) Delgado, M.; Santini, C. C.; Delbecq, F.; Baudouin, A.; De Mallmann, A.; Prestipino, C.; Norsic, S.; Sautet, P.; Basset, J.-M. Characterization of Surface Hydride Hafnium Complexes on Alumina by a Combination of Experiments and DFT Calculations. *J. Phys. Chem. C* **2011**, *115* (14), 6757–6763. <https://doi.org/10.1021/jp200111x>.
- (43) Motta, A.; Szeto, K. C.; Taoufik, M.; Nicholas, C. P. Energetic Pathways and Influence of the Metallacyclobutane Intermediates Formed during Isobutene/2-Butene Cross-Metathesis over WH₃/Al₂O₃ Supported Catalyst. *Catal. Sci. Technol.* **2016**, *6* (10), 3386–3393. <https://doi.org/10.1039/c5cy02154e>.
- (44) Digne, M.; Sautet, P.; Raybaud, P.; Euzen, P.; Toulhoat, H. Hydroxyl Groups on Gamma-Alumina Surfaces: A DFT Study. *J. Catal.* **2002**, *211* (1), 1–5. <https://doi.org/10.1006/jcat.2002.3741>.
- (45) Raybaud, P.; Digne, M.; Iftimie, R.; Wellens, W.; Euzen, P.; Toulhoat, H. Morphology and Surface Properties of Boehmite (Gamma-AlOOH): A Density Functional Theory Study. *J. Catal.* **2001**, *201* (2), 236–246. <https://doi.org/10.1006/jcat.2001.3246>.
- (46) Mazoyer, E.; Trebosc, J.; Baudouin, A.; Boyron, O.; Pelletier, J.; Basset, J.-M.; Vitorino, M. J.; Nicholas, C. P.; Gauvin, R. M.; Taoufik, M.; Delevoye, L. Heteronuclear NMR Correlations To Probe the Local Structure of Catalytically Active Surface Aluminum Hydride Species on Gamma-Alumina. *Angew. Chem. Int. Ed.* **2010**, *49* (51), 9854–9858. <https://doi.org/10.1002/anie.201004310>.
- (47) Taoufik, M.; Le Roux, E.; Thivolle-Cazat, J.; Coperet, C.; Basset, J.-M.; Maunders, B.; Sunley, G. J. Alumina Supported Tungsten Hydrides, New Efficient Catalysts for Alkane Metathesis. *Top. Catal.* **2006**, *40* (1–4), 65–70. <https://doi.org/10.1007/s11244-006-0108-4>.
- (48) Joubert, J.; Delbecq, F.; Sautet, P.; Le Roux, E.; Taoufik, M.; Thieuleux, C.; Blanc, F.; Coperet, C.; Thivolle-Cazat, J.; Basset, J.-M. Molecular Understanding of Alumina Supported Single-Site Catalysts by a Combination of Experiment and Theory. *J. Am. Chem. Soc.* **2006**, *128* (28), 9157–9169. <https://doi.org/10.1021/ja0616736>.
- (49) Pelletier, J.; Espinas, J.; Vu, N.; Norsic, S.; Baudouin, A.; Delevoye, L.; Trebosc, J.; Le Roux, E.; Santini, C.; Basset, J.-M.; Gauvin, R. M.; Taoufik, M. A Well-Defined Silica-Supported Aluminium Alkyl through an Unprecedented, Consecutive Two-Step

- Protonolysis-Alkyl Transfer Mechanism. *Chem. Commun.* **2011**, 47 (10), 2979–2981. <https://doi.org/10.1039/c0cc04986g>.
- (50) Krizan, M.; Honzicek, J.; Vinklarek, J.; Ruzickova, Z.; Erben, M. Titanocene(III) Pseudohalides: An ESR and Structural Study. *New J. Chem.* **2015**, 39 (1), 576–588. <https://doi.org/10.1039/c4nj01404a>.
- (51) Blanckenberg, A.; Malgas-Enus, R. Olefin Epoxidation with Metal-Based Nanocatalysts. *Catal. Rev. Sci. Eng.* **2019**, 61 (1), 27–83. <https://doi.org/10.1080/01614940.2018.1492503>.
- (52) Ma, Z.; Yang, W.; Sun, W.-H. Recent Progress on Transition Metal (Fe, Co, Ni, Ti and V) Complex Catalysts in Olefin Polymerization with High Thermal Stability. *Chin. J. Chem.* **2017**, 35 (5, SI), 531–540. <https://doi.org/10.1002/cjoc.201600720>.
- (53) Gomez Bernal, H.; Cedeno Caero, L.; Finocchio, E.; Busca, G. An FT-IR Study of the Adsorption and Reactivity of Tert-Butyl Hydroperoxide over Oxide Catalysts. *Appl. Catal. A* **2009**, 369 (1–2), 27–35. <https://doi.org/10.1016/j.apcata.2009.08.026>.
- (54) Deubel, D.; Frenking, G.; Gisdakis, P.; Herrmann, W.; Rosch, N.; Sundermeyer, J. Olefin Epoxidation with Inorganic Peroxides. Solutions to Four Long-Standing Controversies on the Mechanism of Oxygen Transfer. *Acc. Chem. Res.* **2004**, 37 (9), 645–652. <https://doi.org/10.1021/ar0400140>.
- (55) Sharpless, K.; Williams, D.; Townsend, J. Mechanism of Epoxidation of Olefins by Covalent Peroxides of Molybdenum(VI). *J. Am. Chem. Soc.* **1972**, 94 (1), 295–296. <https://doi.org/10.1021/ja00756a062>.
- (56) Bach, R.; Wolber, G.; Coddens, B. On the Mechanism of Metal-Catalyzed Epoxidation - A Model for the Bonding in Peroxo Metal-Complexes. *J. Am. Chem. Soc.* **1984**, 106 (20), 6098–6099. <https://doi.org/10.1021/ja00332a067>.
- (57) Manuel Botubol-Ares, J.; Hanson, J. R.; Hernandez-Galan, R.; Collado, I. G. Mild Epoxidation of Allylic Alcohols Catalyzed by Titanium(III) Complexes: Selectivity and Mechanism. *ACS Omega* **2017**, 2 (7), 3083–3090. <https://doi.org/10.1021/acsomega.7b00386>.
- (58) Yu, Y.; Zhu, Y.; Bhagat, M. N.; Raghuraman, A.; Hirsekorn, K. F.; Notestein, J. M.; Nguyen, S. T.; Broadbelt, L. J. Mechanism of Regioselective Ring-Opening Reactions of 1,2-Epoxyoctane Catalyzed by Tris(Pentafluorophenyl)Borane: A Combined Experimental, Density Functional Theory, and Microkinetic Study. *ACS Catal.* **2018**, 8 (12), 11119–11133. <https://doi.org/10.1021/acscatal.8b02632>.
- (59) Parulkar, A.; Spanos, A. P.; Deshpande, N.; Brunelli, N. A. Synthesis and Catalytic Testing of Lewis Acidic Nano Zeolite Beta for Epoxide Ring Opening with Alcohols. *Appl. Catal. A* **2019**, 577, 28–34. <https://doi.org/10.1016/j.apcata.2019.03.009>.
- (60) Caron, M.; Sharpless, K. B. Ti(OiPr)₄ Mediated Nucleophilic Openings of 2,3-Epoxy Alcohols. A Mild Procedure for Regioselective Ring-Opening. *J. Org. Chem.* **1985**, 50, 1560–1563. <https://doi.org/10.1021/jo00209a047>.
- (61) Bradley, D.; Williams, G.; Lawton, M. Aluminium triflate: a remarkable Lewis acid catalyst for the ring opening of epoxides by alcohols. *Org. Biomol. Chem.*, **2005**, 3, 3269–3272. <https://doi.org/10.1039/b508924g>.
- (62) Silvestre-Albero, J.; Domine, M. E.; Jorda, J. L.; Navarro, M. T.; Rey, F.; Rodriguez-Reinoso, F.; Corma, A. Spectroscopic, Calorimetric, and Catalytic Evidences of Hydrophobicity on Ti-MCM-41 Silylated Materials for Olefin Epoxidations. *Appl. Catal. A* **2015**, 507, 14–25. <https://doi.org/10.1016/j.apcata.2015.09.029>.
- (63) Corma, A.; Domine, M.; Ganoa, J. A.; Jorda, J. L.; Navarro, M. T.; Rey, F.; Perez-Pariante, J.; Tsuji, J.; McCulloch, B.; Nemeth, L. T. Strategies to improve the epoxidation activity and selectivity of Ti-MCM-41. *Chem. Commun.*, **1998**, 2211–2212. <https://doi.org/10.1039/A806702C>.

- (64) Activation and reactivity of epoxides on solid acid catalysts. Saikia, L.; Satyarthi, J. K.; Srinivas, D.; Ratnasamy, P. *J. Catal.* **2007**, 252, 148-160. <https://doi.org/10.1016/j.jcat.2007.10.002>.
- (65) Organic reactions at alumina surfaces. Displacement reactions effected by alcohols, thiols, and acetic acid on dehydrated alumina. Posner, G. A.; Rogers, D. A.; Kinzig, C. M.; Gurria, G. M. *Tetrahedron letters*, **1975**, 3597-3600. [https://doi.org/10.1016/S0040-4039\(00\)91333-9](https://doi.org/10.1016/S0040-4039(00)91333-9).
- (66) Organic reactions at alumina surfaces. Mild and selective opening of arene and related oxides by weak oxygen and nitrogen nucleophiles. Posner, G. A.; Rogers, D. Z. *J. Am. Chem. Soc.* **1977**, 99, 8214–8218. <https://doi.org/10.1021/ja00467a014>.
- (67) Knözinger, H.; Köhne, R. Dehydration of Alcohols over Alumina. 1. Reaction Scheme. *J. Catal.* **1966**, 5 (2), 264–270. [https://doi.org/10.1016/S0021-9517\(66\)80007-6](https://doi.org/10.1016/S0021-9517(66)80007-6).
- (68) Roy, S.; Mpourmpakis, G.; Hong, D.-Y.; Vlachos, D. G.; Bhan, A.; Gorte, R. J. Mechanistic Study of Alcohol Dehydration on Gamma-Al₂O₃. *ACS Catal.* **2012**, 2 (9), 1846–1853. <https://doi.org/10.1021/cs300176d>.
- (69) Dufaud, V.; Basset, J. M. Catalytic Hydrogenolysis at Low Temperature and Pressure of Polyethylene and Polypropylene to Diesels or Lower Alkanes by a Zirconium Hydride Supported on Silica-Alumina: A Step Toward Polyolefin Degradation by the Microscopic Reverse of Ziegler-Natta Polymerization. *Angew. Chem., Int. Ed.* **1998**, 37, 806–810. [https://doi.org/10.1002/\(SICI\)1521-3773\(19980403\)37:6<806::AID-ANIE806>3.0.CO;2-6](https://doi.org/10.1002/(SICI)1521-3773(19980403)37:6<806::AID-ANIE806>3.0.CO;2-6).
- (70) Mortensen, J. J.; Parrinello, M. J. A Density Functional Theory Study of a Silica-Supported Zirconium Monohydride Catalyst for Depolymerization of Polyethylene. *Phys. Chem. B* **2000**, 104 (13), 2901–2907. <https://doi.org/10.1021/jp994056v>.

TOC:

Titanium hydride species supported onto silica, silica-alumina and alumina were prepared by the Surface Organometallic Chemistry approach and characterized. They were studied for three important reactions in petrochemistry: epoxidation of 1-octene, depolymerization of a Fischer-Tropsch wax and polymerization of ethylene.

